Journal of the Korean Nuclear Society
Volume 29, Number 5, pp. 361~367, October 1997

Analysis of Phase Separation by Thermal Aging in Duplex Stainless Steels by Magnetic Methods

Sunki Kim, Wonmok Jae, and Yongsoo Kim
Hanyang University
17 Haengdang-Dong, Sungdong-Ku, Seoul, 133-791, Korea

(Received January 14, 1997)

Abstract

The phase separation in ferrite phase of duplex stainless steel is the primary cause of thermal aging embrittlement of the LWR primary pressure boundary components. In this study the phase separation of simulated duplex stainless steel was detected by Mössbauer spectroscopy and magnetic property analysis by VSM(Vibrating Specimen Magnetometer). The simulated duplex stainless steels, Fe-Cr binary, Fe-Cr-Ni ternary, and Fe-Cr-Ni-Si quarternary alloys, were aged at 370 and 400℃up to 5,340 hours. It was observed from Mössbauer spectra analysis that internal magnetic field increases with aging time and from VSM that the specific saturation magnetization and Curie temperature increase with aging time. These results are indicative that phase separation into Fe-rich region and Cr-rich region is caused by thermal aging in the temperature range of 370~400℃. In cases of specimens containing Ni, the increase of specific saturation magnetization is much higher. This implies that Ni seems to promote Fe-Cr interdiffusion, which accelerates the phase separation into Fe-rich α phase and Cr-rich α' phase.

1. Introductions

Cast duplex stainless steels, composed of austenite and ferrite phases, are extensively used for primary pressure boundary components such as primary coolant pipe, valves, pump casings, and weld filler metal in LWRs. The ferrite phase in the duplex structure increases tensile strength and improves weldability, resistance to stress corrosion cracking, and soundness of castings. The superior properties of the cast stainless steels result primarily from the presence of the ferrite phase in the duplex structure. On the other hand, it is known that ferritic stainless steels become brittle owing to the precipitaion of the α' phase when exposed to temperatures in the range of 300~500℃ for a long time [1-3].

It was reported that primary pressure boundary components such as hot leg elbow, main valve, and recirculation pump cover decommissioned from Ringhals Unit 2, Shippingport PWR, and KRB BWR had suffered severe degradation in impact properties [4, 5]. The significant deterioration in which the cast stainless steels were aged at temperatures of 300~450℃ up to 70,000h has been supported by recent studies [6,7]. Since the real aging of the components at the end of lifetime at reactor operating temperatures (280~330℃) cannot be reproduced in the laboratory, it is customary to simulate it by accelerated aging at 400℃. Therefore, it is important to validate that the mechanisms of the aging embrittlement are

identical for the accelerated aging and reactor operating conditions. Fortunately, they are believed to be similar and it has been demonstrated that the embrittlement of aged cast stainless steels is attributed primarily to Cr-rich α' precipitation by spinodal decomposition [7,8].

In the previous investigations, transmission electron microscopy (TEM), small angle neutron scattering (SANS), and atom probe field ion microscopy (APFIM) results show that several metallurgical processes such as the precipitation of G phase, γ_2 phase, α' phase by spinodal decomposition, and $M_{23}C_6$ formation can be the causes of aging embrittlement in the duplex stainless steel [6-8]. Microhardness analysis, toughness recovery, and microstructural evolution of aged specimens following an annealing treatment at 550℃ showed that the primary mechanism for the thermal aging embrittlement is the spinodal decomposition of the ferrite [9]. Recently, non-destructive methods such as magnetic properties analysis by Mössbauer spectrometer and electrochemical properties analysis are applicated to estimate the degree of thermal aging embrittlement of duplex stainless steels [10].

In the present study, primarily the phase separation into α phase and α' phase in the simulated duplex stainless steels is experimentally detected by Mössbauer spectra analysis. Secondly Curie temperature and variations in the specific saturation magnetization of several simulated duplex stainless steels are investigated to analyze phase separation by using VSM.

2. Experiments

Mössbauer spectroscopy for duplex stainless steel is undesirable because of the fact that austenite phase in dulpex structure is paramagnetic and obscures the detection of the paramagnetic α' phase. Therefore, single phase ferrite alloys such as Fe-Cr binary, Fe-Cr-Ni ternary, and Fe-Cr-Ni-Si quarternary alloy were used to analyze phase separation with Mössbauer spectrometer and VSM. Their chemical compositions are given in Table 1. Specimens were cut into 1cm×1cm thin square plates, aged at 370 and 400℃ in evacuated Pyrex tube, and then abraded to the thickness of 0.06~0.08 mm for Mössbauer spectra analysis.

Table 1. Compositions of Thermally-aged Specimens

(unit: wt.%)

Heat	Cr	Ni	Si	Fe
HY1	25	–	–	Bal.
HY2	30	–	–	Bal.
HY3	30	5	–	Bal.
HY4	30	5	2	Bal.

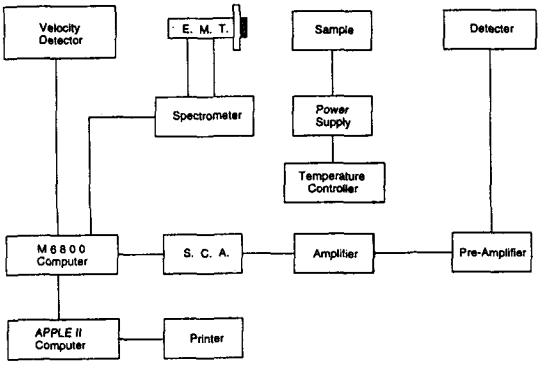

Fig. 1. Schematic Diagram of Mössbauer Spectrometer

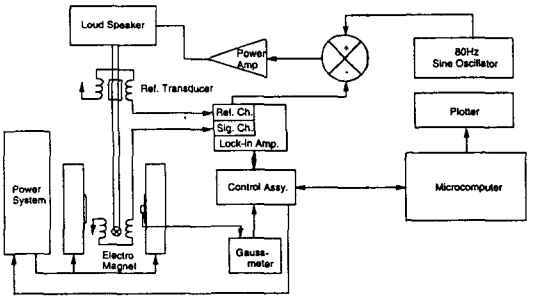

Fig. 2. Schematic Diagram of Vibrating Specimen Magnetometer(VSM)

To detect the phase separation into Fe-rich regions and Cr-rich regions, Mössbauer spectrometer and vibrating specimen magnetometer (VSM) were used. The schematic diagrams of these apparatuses are

shown in Figure 1 and 2, respectively. The operating principles of Mössbauer spectrometry are as follows. Electric signal from Motorola 6800 computer operates spectrometer, which drives linear drive motor. This causes γ-rays from ^{57}Co source attatched to the drive motor to get Doppler energy. The γ-rays pass through the specimen and arrive at detector, then ionize mixture gas of Kr-CO_2 in the detector. Then electric energy is provided for the gas mixture by applying high voltage of 1,880V. After electric signals of ionized gas mixture are amplified by pre-amplifier and amplifier, the signals corresponding to 14.4 keV are detected and saved by data acquisition system. Mössbauer spectra were obtained in absorption geometry at room temperature using an Austin S-600 spectrometer and the relative absorption was plotted with respect to the source velocity. Positive velocity corresponds to the source moving towards the absorber, while zero velocity is set to the centroid of the spectrum of Fe-metal. r-source in the Mössbauer spectroscopy was 10mCi ^{57}Co electrodeposited in 6μ m-thick ^{103}Rh. Doppler velocity between the source and the absorber was controlled to $\pm$12mm/sec.

VSM analysis is based on the flux change in a coil when the specimen vibrates around the coil. The specimen is attached to the end of a rod as can be seen in Figure 2. Current through the loudspeaker vibrates the rod and specimen at 80 Hz and with an amplitude of about 0.1 mm in a direction at right angle to the magnetic field. The oscillating magnetic field of the specimen induces an alternating E.M.F in the detection coils. The oscillating magnetic field of the reference specimen also induces an another E.M.F in two reference coils. The voltage signals from two sets of coils are compared, and the difference is proportional to the magnetic moment of the specimen. Saturation magnetization with temperature was measured to estimate Curie temperature. Applied magnetic field for the saturation magnetization measurement in the vibrating specimen magnetometer(VSM) was 5kOe.

3. Results and Discussion

In the first part, analysis of Mössbauer spectrum was carried out to verify the phase separation into Fe-rich and Cr-rich regions in aged duplex stainless steels. In the spectrum six peaks of γ-rays by ^{57}Fe nuclei are observed when these nuclei are in ferromagnetic environments such as in α-iron below the Curie temperature. If the ^{57}Fe nucleus is in a paramagnetic environment, then a single paramagnetic peak, located near zero velocity, is observed.

If both ferromagnetic and paramagnetic phases co-exist in the alloy, six ferromagnetic peaks and a single paramagnetic peak near zero velocity are superposed in the spectrum. The spacing between the first peak(V1) and the sixth peak(V6) is proportional to the internal field of the iron nucleus.

The field can be characterized by the distance between two outmost ferromagnetic peaks :

$$H = 330(V6 - V1)/10.657 \quad (1)$$

The value of 330 corresponds to the internal field around ^{57}Fe nucleus in pure Fe at room temperature and 10.657 in the denominator corresponds to the conversion of the difference between the first (V1) and the last peak position (V6) into doppler velocity in Mössbauer spectrum. The peak positions were determined by Lorentzian curve fitting. The spectrum changes of specimens, HY2 (70Fe-30Cr), with aging time up to 5,064 hours at 370℃ are shown in Figure 3. It turns out that appreciable paramagnetic phase was not formed even after 5,064 hour aging since there is no peak near zero velocity.

Based on equation (1) the internal field in the specimen were calculated and plotted in Figure 4. This shows that the internal field is increasing with aging time, which obviously means that ferromagnetism of the steel is increasing. When Cr leaves the α phase, the number of Cr atoms neighboring Fe atoms decreases and concomitantly Fe neighbors increase. This causes the internal field increase by Fe nuclei in

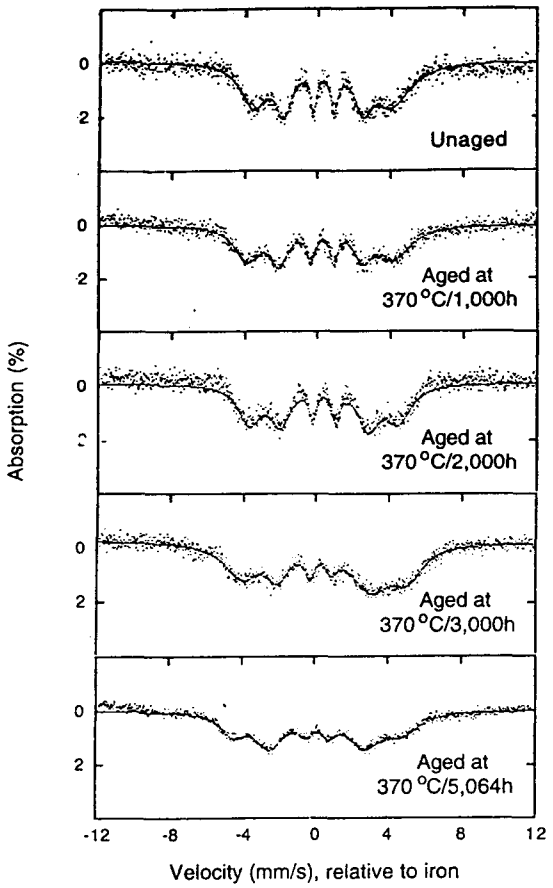

Fig. 3. Mössbauer Spectra for Thermally-aged HY2 Specimen at 370℃

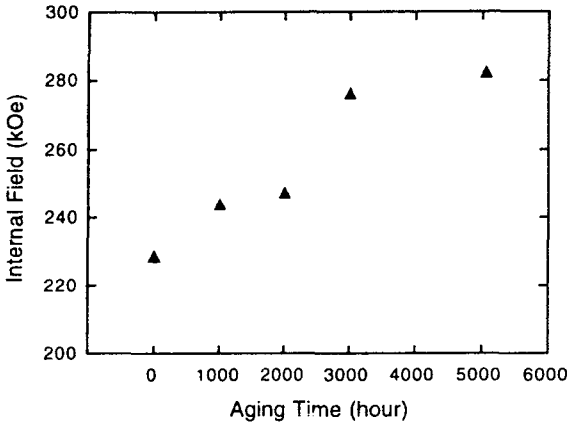

Fig. 4. Internal Field for Thermally-aged HY2 Specimen at 370℃

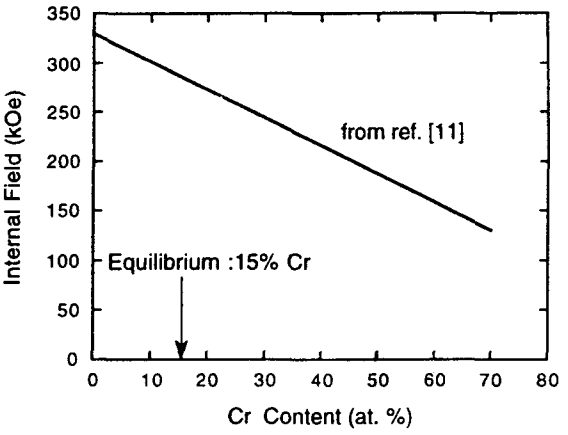

Fig. 5. Internal Field vs. Cr Content for Binary Fe-Cr Alloys

the ferromagnetic α-phase. In Mössbauer spectrum analysis, in actual, the contribution of reduced ^{57}Fe atoms in Cr-rich region is much less than that of increased ^{57}Fe atoms in Fe-rich region in the total field change, since the spectrum picks up only Fe signal. This brings about the net increase in the internal field change, since the spectrum picks up only Fe sig- Fe-rich region and Cr-rich region.

This is supported by Figure 5 drawn from Johnson et al.' report [11] showing that the internal field is decreasing with increasing Cr content. Almost identical curve can be drawn from the data of Yamamoto [12], De Nys and Gielen [13], and Roy and Solly [14]. The intenal field of 280kOe after 5,064 hour aging in Figure 4 corresponds to about 20 at.% Cr (18 wt.% Cr), which is 5 at.% larger than the equilibrium Cr content in the α-phase. This is indicative that equilibrium α'phase was not formed yet and phase separation is proceeding.

Secondly, the magnetic property change of the steels was identified by the measurement of Curie temperature, transition temperature of ferromagnetism and paramagnetism. For the estimation of Curie temperature, saturation manetizations of thermally aged HY2 specimens at 400℃ were measured under vacuum condition as a function of measured tempera-

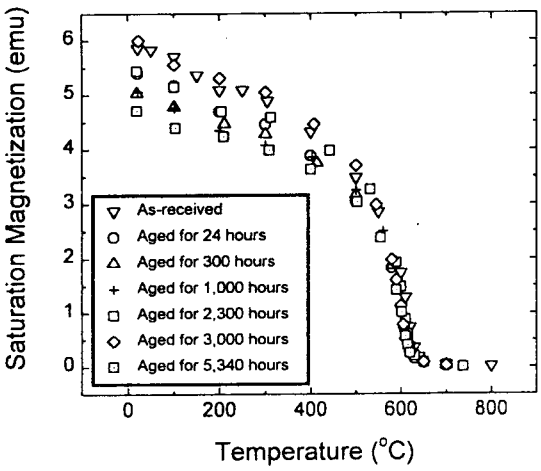

Fig. 6. Saturation Magnetization of Thermally-aged HY2 Specimen at 400℃ as a Function of Measured Temperature

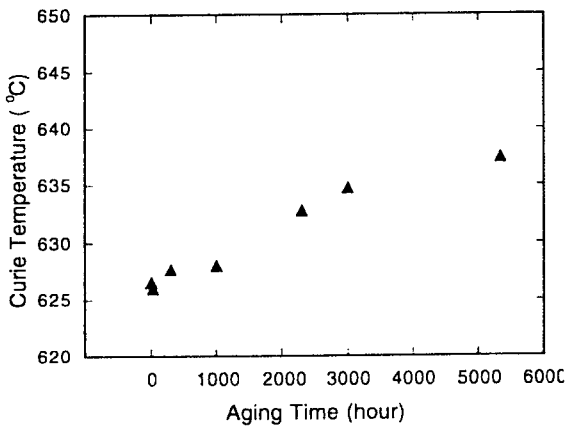

Fig. 7. Curie Temperature of Thermally-aged HY2 Specimen at 400℃ as a Function of Measured Temperature

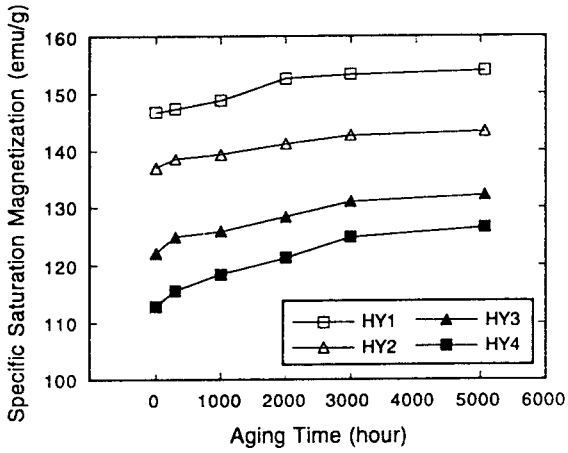

Fig. 8. Specific Saturation Magnetization as a Function of Aging Time at 370℃

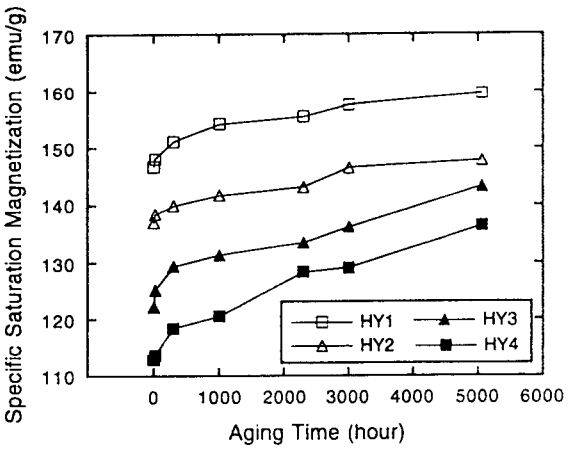

Fig. 9. Specific Saturation Magnetization as a Function of Aging Time at 400℃

ture (Figure 6). Then Curie temperatures were derived from the figure by least square curve fitting of the three data points whose slope is maximum. They are plotted in Figure 7. It shows that Curie temperature increases with aging time, which confirms that ferromagnetic property of the specimen increases, therefore the phase separation is proceeding.

Last, variations in the specific saturation magnetization of several simulated duplex stainless steels, HY1 through HY4, were measured with aging time to investigate the effects of alloying elements at 370 and 400℃. Specific saturation magnetization is very useful to analyze phase change in magnetic materials, because it is not almost dependent to local strain and lattice defects in materials but dependent to alloy composition and distribution of phases whose magnetic properties are different from each other. They are shown in Figure 8 and 9, respectively. It

can be seen that specific saturation magnetization increases with increasing Fe content. This is due to ferromagnetic property of Fe. Distribution of specfic saturation magnetization is in order of HY1(containing 75%Fe)>HY2(70%Fe)>HY3(65%Fe)>HY4 (63%Fe). Increase in specific saturation magnetization is also observed for all specimens with increasing aging time. This fact is indicative that Fe content increases in α phase with aging time, that is, phase separation into Fe-rich regions and Cr-rich regions is proceeding with aging time. This is obviously due to the enhanced ferromagnetic property of Fe caused by the phase separation. This can be explained by molecular theory and exchange energy of ferromagnetic elements. However specific saturation magnetization did not saturate yet, but increases continuously with aging time. This suggests that the matrix did not separate into Fe-rich phase and Cr-rich phase completely and approach the equilibrium state. This result is in accord with that from Mössbauer spectra analysis.

Much higher increase in specific saturation magnetization is especially observed for HY3 and HY4 specimens containing Ni compared with HY1 and HY2 without Ni. In general, the rate of spinodal decomposition in ternary alloy is controlled by the interdiffusion coefficient. The influence of Ni on Fe-Cr interdiffusion seems to play an important role. This result is in accord with Solomon's result [15] by Mössbauer spectra analysis. but, there is no accepted mechanism for this accelerating effect of Ni. The effect of Si alloying element was also investigated to examine whether it promotes phase separation by clustering with Ni (so-called G phase) or not. But, appreciable differences in specific saturation magnetization between HY3 (not containing Si) and HY4 (containing Si) were not observed within the Si composition of 2%.

4. Conclusions

Undesirable phase separation by so-called spinodal decomposition into Fe-rich and Cr-rich phase is the primary cause of the embrittlement in primary pressure boundary components at LWR operating temperatures. Mössbauer spectroscopy and VSM analysis have verified the phase separation in the aged duplex stainless steels. From the experimental results that internal field, specific saturation magnetization, and Curie temperature increase with aging time, it is confirmed that the ferrite phase separates into Fe-rich α phase and Cr-rich α' phase by thermal aging in the temperature range of 370~400℃.

In cases of specimens containing Ni, the increase of specific saturation magnetization is much higher. This implies that Ni seems to promote Fe-Cr interdiffusion, which accelerates the phase separation into Fe-rich α phase and Cr-rich α' phase.

Acknowledgement

The authors gratefully acknowledge the financial support of the Korea Science and Engineering Foundation. Especially the authors express our gratitute to Dr. Junsang Park at KINS for specimen supply and discussion for the present study.

References

1. H.M. Jung, *ASME PVP* **171**, 111 (1989)
2. C. Jasson, *Proc. Fontevraud* II *Int'l. Symp.* Fontevraud, France (1990)
3. O.K. Chopra and H.M. Jung, *Nucl. Eng. and Desg.*, **89**, 305 (1985)
4. H.M. Jung and T.R. Leak, International Workshop on *Intermediate Temp. Embrittlement Process in Duplex Stainless Steel,* Oxford, England (1989)
5. O.K. Chopra and H.M. Jung, *Proc. 16th Water Reactor Safety Information Meeting,* Gaithersburg (1988)
6. O.K. Chopra and H.M. Chung, *Proc. 3rd Int.*

Symp. on Environmental Degradation of Materials in Nuclear Power Systems-Water Reactors, Monterey, USA (1988)

7. H.M. Jung and T.R. Leax, *Material Science and Technology*, **6**, 249 (1990)
8. M.K. Miller and J. Bentley, *Material Science and Technology*, **6**, 285 (1990)
9. J.E. Brown, G.D.W. Smith, P.H. Pumphrey, and M.K. Miller, *Proc. 5th Int. Symp. on Environmental Degradation of Materials in Nuclear Power Systems-Water Reactors*, Monterey, USA (1991)
10. J.S. Park, Thesis of Ph. D, Korea Advanced Institute of Science and Technology (1995)
11. C.E. Johnson, M.S. Ridout, and T.E. Cranshaw, Proc. *Phys. Soc.*, **81**, 1079 (1963)
12. H. Yamamoto, Japan *J. Appl. Phys.*, **3**, 745 (1964)
13. T. De Nys and P.M. Gielen, *Metall. Trans.*, **2**, 1423 (1971)
14. R.B. Roy and B. Solly, *Scand. J. Metallurgy*, **2**, 243 (1973)
15. H.D. Solomon, L.M. Levinson, *Acta. Met.*, **26**, 429 (1978)